



Design of a Lightweight Deployable Planar Parallel Manipulator with Tape Spring Mechanism

Yaqi Tang, Huayong Zheng, Lei Tang, Yan Peng, Huayan Pu
and Yi Yang

EasyChair preprints are intended for rapid
dissemination of research results and are
integrated with the rest of EasyChair.

January 9, 2020

Design of a lightweight deployable planar parallel manipulator with tape spring mechanism

Yaqi TANG^a, Huayong ZHENG^b, Lei TANG^a, Yan PENG^a, Huayan PU^a, Yi YANG^{a,1}

^a*School of Mechatronic Engineering and Automation, Shanghai University, Shanghai 200444, PR China.*

^b*Aerospace System Engineering Shanghai, Shanghai 201109, PR China.*

Abstract. A tape spring is a thin-walled, open cylindrical structure with a natural transverse curvature. The localized folds in the tape spring can be served as revolute joints, and the unfolded straight segments served as links. If an external torque is imposed on the fold, the fold can slide along the tape spring. Inspired by that, a novel deployable planar parallel manipulator composed of one tape spring and two driving pulleys is proposed for the first time. The kinematics and dynamics models are derived. Within consideration of buckling stability of the tape spring, the workspace of the moving platform is investigated. At last, the prototype is manufactured and experimented to validate the presented design and analysis. With the virtue of low masses, simple mechanics and high efficiency of enfoldment, potential application of the deployable parallel manipulator for unmanned aerial vehicle (UAV) is discussed.

Keywords. Deployable parallel manipulator, Tape spring, Kinematics, Dynamics, Workspace.

1. Introduction

Deployable mechanisms can generally vary their shapes significantly. They can fold into a small configuration for storage and expand to a much larger immovable structure for working. Examples include the scissor-like-mechanisms (SLiMs)[1], Wohlhart's polyhedral star transformers[2], Hoberman's polyhedral mechanisms[3], Bricard's and Bennett's derived mechanisms[4][5], origami-derived mechanisms[6]. Some researchers introduce the concept of deployable mechanisms into the design of the manipulator. In 2009, Dai and Wang invented a metamorphic hand with a foldable palm[7]. In 2016, Chablat and Rolland designed a parallel robot with a set of networked scissors that reduced the swept volume of the kinematic chains[8]. In 2017, Gonzalez and Asada proposed a 6-DOF parallel robot with a triple scissor extender that can be applied to aircraft assembly[9]. In 2019, Yang et al proposed a dual scissor-like mechanism (D-SLiM), and designed certain types of parallel lower-mobility manipulators [10][11].

A tape spring is a thin-walled, open cylindrical structure with a natural transverse curvature. It has some remarkable properties[12], such as being stiff before buckling while being compliant after buckling, having a constant fold radius[13] and constant moment after buckling[14]. The tape spring is widely used in the space deployable structure, such as deployable booms, deployable antenna or flexure hinge. The

¹ Corresponding Author. yiyangshu@t.shu.edu.cn

deployable structures with tape springs have advantages of low masses, simple mechanics, high efficiency of enfoldment, and no mechanical joints.

To enlarge the workspace, save storage space and reduce weight, we introduce the tape spring into the design of the deployable manipulator. A novel deployable planar parallel manipulator with tape spring mechanism has been invented. The rest of the paper is organized as follows. In Section 2, the structure of this deployable parallel manipulator is described. In Section 3, the kinematics and singularities are discussed. In Section 4, the dynamic model is established. In Section 5, the prototype is manufactured and experimented. And a potential application of this deployable planar parallel manipulator with tape spring mechanism is discussed.

2. Mechanism design

In tape spring, the localized folds serve as revolute joints, and the unfolded straight segments serve as links. A fold and its adjacent straight segments can be viewed as a two rigid-links with a revolute joint, as shown in Figure 1a. If an external torque is imposed on the fold, the fold can slide along the tape spring. The fold and its adjacent straight segments of the tape spring can be regarded as a RP-R-PR mechanism.

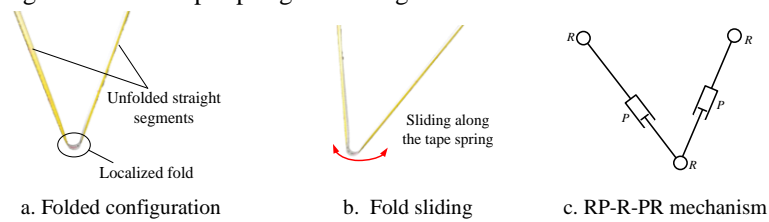


Figure 1. Transformation of tape spring and kinematic representation.

Inspired by the above conception, a novel deployable planar parallel manipulator composed of a tape spring and 2 driving pulleys is proposed for the first time, as shown in Figure 2. One driving pulley D_1 is placed on the end, to extend or shorten the total length of the tape spring. The other driving pulley D_3 is placed on the fold of the tape spring. The 3 driven pulleys are paired under the driving pulley D_3 . The driving and driven pulleys flatten the tape spring to reduce the resistant torsion of the fold when the driving pulley D_3 moves along the tape spring. The position of the fold can be controlled by driving pulleys D_1 and D_3 .

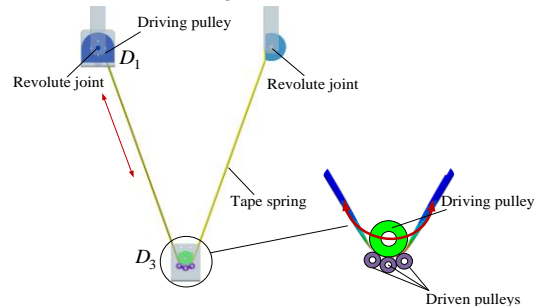


Figure 2. Schematic diagram of deployable parallel mechanism with tape spring.

The detailed design of an ultralight deployable planar parallel manipulator with tape spring is shown in Figure 3. The deployable mechanism involves an end drive assembly, which is hinged with the T-shaped connection. The end drive assembly can extend or shorten the length of the total length of the tape spring. The other end of the tape spring is hinged with the T-shaped connection. The middle drive assembly is placed on the fold of the tape spring. Through the rolling of the pulley, the middle drive assembly can move along the tape spring. There are a steering motor and a gripper below the middle drive assembly. By controlling the end and the middle drive assemblies, the position of the gripper can be determined. The orientation of the gripper can be controlled by the steering motor between the middle drive assembly and the gripper. Due to the large range of motion of the tape spring, such planar parallel manipulator is capable of being collapsed for storage (as shown in Figure 3b) and deployed in the work stage (as shown in Figure 3a).

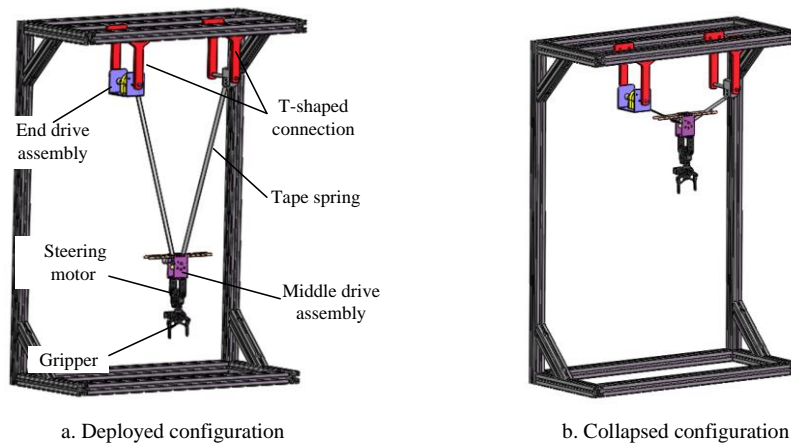


Figure 3. Detailed structure of deployable parallel manipulator.

2.1. End drive assembly

Exploded and assembled renderings of the end drive assembly are shown in Figure 4. The end drive assembly involves U-shaped frame and hub mechanism. Fix the tape spring on the hub, and then press the gland at both ends. The mini motor is connected with the hub through the flange.

The design of the step shaft at both ends of the U-shaped frame can realize the free rotation of the end drive assembly. The motor drives the hub to rotate to realize the deploying and collapsing of the planar parallel manipulator with tape spring mechanism.

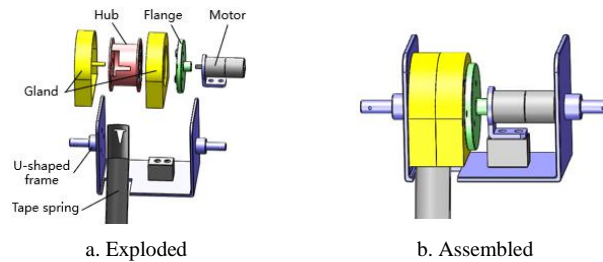


Figure 4. End drive assembly.

2.2. Middle drive assembly

As shown in Figure 5, they are exploded and assembled renderings of the middle drive assembly. The middle drive assembly involves U-shaped frame and gripper. The motor is fixed to the U-shaped frame by the connection, and the shaft and the driving pulley are jointed by the pin.

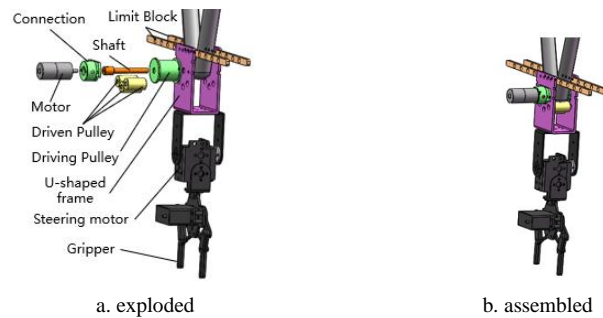


Figure 5. Middle drive assembly.

The driving pulley is designed with a groove. Three driven pulleys are evenly placed in the groove to press the tape spring, which can effectively flatten the tape spring in the movement process. The two limit blocks can limit the offset of the tape spring during the movement. In addition, the gripper has two degrees of freedom. If the U-shaped frame tilts during the movement, the orientation of the gripper can be rotated by controlling the steering motor between the middle drive assembly and the gripper.

3. Kinematics and singularities

As shown in Figure 6, D_1 and D_3 represent the drive pulleys. D_2 represent the passive joint. The connection between D_1 and D_3 , D_3 and D_2 is a tape spring. To simplify the kinematic model, the effects of the radius of the pulleys on the position of D_3 are ignored. The initial lengths of the tape spring between D_1 and D_3 , D_3 and D_2 are both l_0 . If the drive pulleys D_1 and D_3 rotate the angles θ_1 and θ_2 respectively, the lengths of the tape spring between D_1 and D_3 , D_3 and D_2 are $l_0 + r_1\theta_1 - r_2\theta_2$ and $l_0 + r_2\theta_2$.

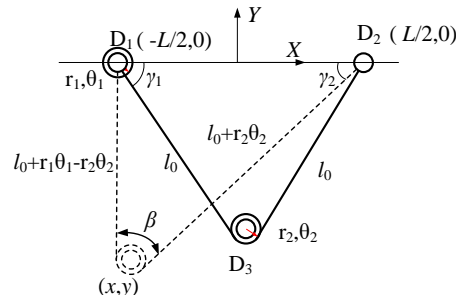


Figure 6. Kinematic model.

According to the geometrical relationship in Figure 6, the following conditions are established

$$\begin{cases} \sqrt{(x+L/2)^2 + y^2} = l_0 + r_1\theta_1 - r_2\theta_2 \\ \sqrt{(x-L/2)^2 + y^2} = l_0 + r_2\theta_2 \end{cases} \quad (1)$$

Squaring both sides of the above equation and subtracting the first formula to the second one, we can obtain

$$x = \frac{1}{2L}(r_1\theta_1 - 2r_2\theta_2)(2l_0 + r_1\theta_1) \quad (2)$$

Substituting Eq. (2) into the first formula of Eq. (1), it leads to

$$y = -\sqrt{(l_0 + r_2\theta_2)^2 - (x-L/2)^2} \quad (3)$$

By Eqs. (2) and (3), the position of D_3 can be quickly solved. Then, differentiating Eq. (1) with respect to time, the velocity equations are obtained as follows

$$\begin{bmatrix} \cos \gamma_1 & -\sin \gamma_1 \\ -\cos \gamma_2 & -\sin \gamma_2 \end{bmatrix} \begin{bmatrix} \dot{x} \\ \dot{y} \end{bmatrix} = \begin{bmatrix} r_1 & -r_2 \\ 0 & r_2 \end{bmatrix} \begin{bmatrix} \dot{\theta}_1 \\ \dot{\theta}_2 \end{bmatrix} \quad (4)$$

Where:

$$\begin{aligned} \cos \gamma_1 &= \frac{x+L/2}{l_1}, \quad \sin \gamma_1 = -\frac{y}{l_1}, \quad \cos \gamma_2 = -\frac{x-L/2}{l_2}, \quad \sin \gamma_2 = -\frac{y}{l_2}, \\ l_1 &= \sqrt{(x+L/2)^2 + y^2}, \quad l_2 = \sqrt{(x-L/2)^2 + y^2} \end{aligned} \quad (5)$$

Eq. (4) can further be transformed to

$$J_k \begin{bmatrix} \dot{x} \\ \dot{y} \end{bmatrix} = \begin{bmatrix} \dot{\theta}_1 \\ \dot{\theta}_2 \end{bmatrix} \quad (6)$$

where the Jacobian matrix J_k is

$$J_k = \begin{bmatrix} (\cos \gamma_1 - \cos \gamma_2) / r_1 & -(\sin \gamma_1 + \sin \gamma_2) / r_1 \\ -\cos \gamma_2 / r_2 & -\sin \gamma_2 / r_2 \end{bmatrix} \quad (7)$$

The determinant of the Jacobian matrix J_k is

$$|J_k| = -\sin(\gamma_1 + \gamma_2) / (r_1 r_2) \quad (8)$$

Observing Eq. (8), it's found that the mechanism is in singularity, when $\gamma_1 + \gamma_2 = 0, \pi$. The corresponding singular configurations are presented, as shown in Figure 7.

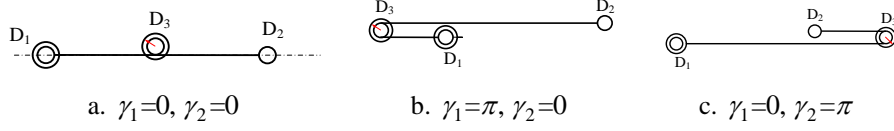


Figure 7. The singularities of the deployable manipulator.

4. Dynamic model

The dynamic model is derived in this section. Taking m as the mass of the moving platform at D_3 , the moving platform is simplified into the mass point which are assumed to be in the center of the pulley D_3 . Because the tape spring is very light, its mass is neglected in this model. The simplified dynamics equation can be written as

$$\begin{bmatrix} M_1 \\ M_2 \end{bmatrix} = (J_k^T)^{-1} \begin{bmatrix} f_x \\ f_y \end{bmatrix} = (J_k^T)^{-1} \left(-m \begin{pmatrix} \ddot{x} \\ \ddot{y} \end{pmatrix} + m \begin{pmatrix} g_x \\ g_y \end{pmatrix} + \begin{pmatrix} F_x \\ F_y \end{pmatrix} \right) \quad (9)$$

Considering

$$\begin{bmatrix} \ddot{x} \\ \ddot{y} \end{bmatrix} = J_k^{-1} \left(\begin{pmatrix} \ddot{\theta}_1 \\ \ddot{\theta}_2 \end{pmatrix} - \dot{J}_k J_k^{-1} \begin{pmatrix} \dot{\theta}_1 \\ \dot{\theta}_2 \end{pmatrix} \right) \quad (10)$$

and substituting the above equation into Eq. (9), the equation can be rewritten as

$$\begin{bmatrix} M_1 \\ M_2 \end{bmatrix} = -(J_k^T)^{-1} m J_k^{-1} \begin{pmatrix} \ddot{\theta}_1 \\ \ddot{\theta}_2 \end{pmatrix} + (J_k^T)^{-1} m J_k^{-1} \dot{J}_k J_k^{-1} \begin{pmatrix} \dot{\theta}_1 \\ \dot{\theta}_2 \end{pmatrix} + (J_k^T)^{-1} m \begin{pmatrix} g_x \\ g_y \end{pmatrix} + (J_k^T)^{-1} \begin{pmatrix} F_x \\ F_y \end{pmatrix} \quad (11)$$

where the derivative of Jacobian matrix \dot{J}_k is

$$\dot{J}_k = \begin{bmatrix} \frac{\dot{x}l_1 - (x+L/2)(\frac{\partial l_1}{\partial x}\dot{x} + \frac{\partial l_1}{\partial y}\dot{y})}{l_1^2 r_1} + \frac{\dot{x}l_2 - (x-L/2)(\frac{\partial l_2}{\partial x}\dot{x} + \frac{\partial l_2}{\partial y}\dot{y})}{l_2^2 r_1} & \frac{\dot{y}l_1 - y(\frac{\partial l_1}{\partial x}\dot{x} + \frac{\partial l_1}{\partial y}\dot{y})}{l_1^2 r_1} + \frac{\dot{y}l_2 - y(\frac{\partial l_2}{\partial x}\dot{x} + \frac{\partial l_2}{\partial y}\dot{y})}{l_2^2 r_1} \\ \frac{\dot{x}l_2 - (x-L/2)(\frac{\partial l_2}{\partial x}\dot{x} + \frac{\partial l_2}{\partial y}\dot{y})}{l_2^2 r_2} & \frac{\dot{y}l_2 - y(\frac{\partial l_2}{\partial x}\dot{x} + \frac{\partial l_2}{\partial y}\dot{y})}{l_2^2 r_2} \end{bmatrix} \quad (12)$$

5. Workspace and simulation

According to Section 3, it's known that the workspace is an ellipse with regard to a given constant total length of the tape spring. The long axis of the ellipse of the workspace is

$$a = (2l_0 + r_1 \theta_{1,\max}) / 2 \quad (13)$$

And the minor axis of the ellipse is

$$b = \sqrt{a^2 - (L/2)^2} \quad (14)$$

Considering that part of the tape spring would bear pressure following the changing of position D_3 , it would lead to buckling of the tape spring, which makes the mechanism invalidation. The workspace should exclude these areas. Assuming the shape of cross-sectional geometry of the tape spring is an arc as shown in Figure 8. r is the radius, t is the wall thickness and α is the angle of the arc edge to the vertical y axis. Based on column buckling theory, the maximum press of the tape spring is

$$P_{\max} = \frac{\pi^2 EI_c}{L^2} \quad (15)$$

Where the second moment of area I_c is

$$I_c = r^3 t \alpha \left(\frac{1}{2} \frac{\sin 2\alpha}{\alpha} + 1 - \frac{2 \sin^2 \alpha}{\alpha^2} \right) \quad (16)$$

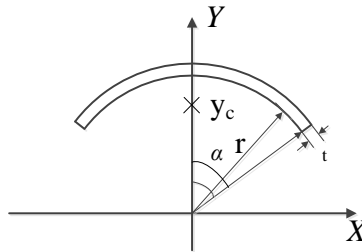


Figure 8. Cross-sectional geometry of tape spring.

To avoid the buckling of the tape spring, the pressure of the tape spring P in the workspace should satisfy, $P < P_{\max}$. Given the length $D_1 D_2 = 365\text{mm}$, the maximum total length of the tape spring $s_{\max} = 1400\text{mm}$, the minimum total length of the tape spring $s_{\min} = 460\text{mm}$, the parameters of the cross-section of the tape spring is $r = 11.5\text{mm}$, $2\alpha = 1.57$ and $t = 0.1\text{mm}$. Young's module of the tape spring is $E = 1.31 \times 10^5 \text{Nmm}^{-2}$. The workspace of this deployable parallel manipulator is calculated and presented in Figure 9.

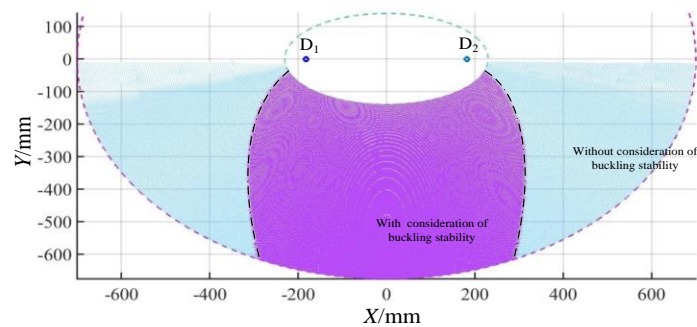


Figure 9. Workspace of the deployable parallel manipulator.

In Figure 9, the light blue area is the space without consideration of buckling stability of the tape spring. The shape of this area is a half of ellipse. Then, considering

the constraint of buckling stability, $P < P_{\max}$, the workspace of the manipulator reduces to the purple area.

Furthermore, the driving torques of the two pulleys are investigated. Given the total mass of the middle drive assembly, steering motor and the gripper is 1kg, the direction of gravity is along $-y$ axis, the influence of the angular velocities and accelerations of the pulleys is neglected. The driving torques are calculated and as shown in Figure 10.

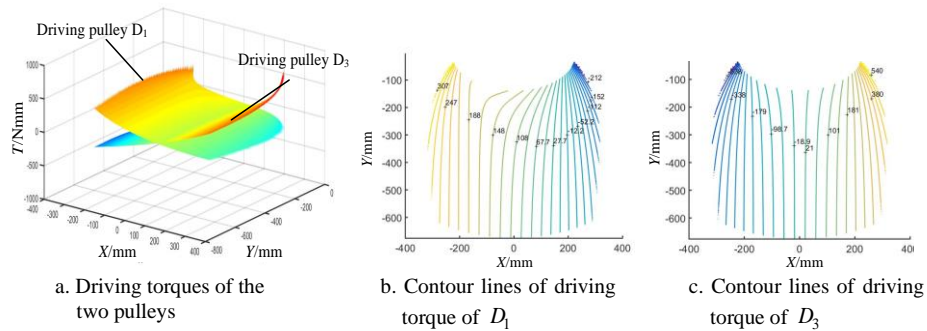


Figure 10. Torques of the two driving pulleys.

From Figure 10, it's known that the maximum driving torque of pulley D_1 is 348Nmm, and the maximum torque of pulley D_3 is 620Nmm. These results provide references for the motor selection. Figures 10b and 10c show that the maximum driving torques are located in the edge of the workspace, while the driving torques in the middle of the workspace are relatively small. Figure 10b shows that the driving torque of pulley D_1 equals zero when the moving platform is positioned at $X=365/2$. And Figure 10c shows the driving torque of pulley D_3 equals zero if the moving platform is positioned at $X=0$. Figure 10c also demonstrates that the distribution of driving torque of pulley D_3 is symmetrical about y-axis.

6. Prototype and motion experiments

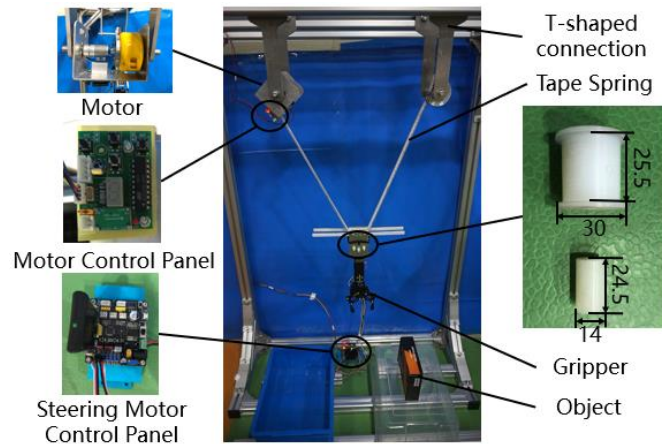


Figure 11. Prototype of planar parallel manipulator with tape spring mechanism.

The 4th INTERNATIONAL WORKSHOP ON FUNDAMENTAL ISSUES,
APPLICATIONS AND FUTURE RESEARCH DIRECTIONS FOR
PARALLEL MECHANISMS / MANIPULATORS / MACHINES,
BELFAST, UK, 25-26 JUNE 2020

As shown in Figure 11, an experimental platform is built with aluminum profiles. The U-shaped frame is installed on the top of the platform, which is made of aluminum alloy. The driving pulley and three driven pulleys are placed tangent to each other, which are made of nylon.

The length of the tape spring is 1400 mm, and the width is 25 mm; the diameter of the driving pulley is 30 mm and the width of the groove is 25.5 mm; the diameter of the driven pulley is 14 mm, and the width is 24.5 mm. By controlling the two motors, the ultralight deployable planar parallel manipulator with tape spring mechanism can move along the x-axis and y-axis.

In this experiment, the T-shaped connection is fixed to the experimental platform, and a 200g box is placed at the bottom. When the two motors are running synchronously, the planar parallel manipulator with tape spring mechanism deploys along the center line, as shown in Figure 12a. As shown in Figure 12b, by controlling the end drive assembly and the middle drive assembly, the manipulator moves to the right during the deploying process. As shown in Figure 12c, when the manipulator moves to the position near the object, the gripper adjusts its orientation by rotating the steering motor, and grasps the object. After grasping the object, the gripper moves to the top of the left blue box, places the object in the blue box, and then retracts to the original position. The motion of the manipulator is continuity and smooth. The moving process is shown in Figure 12d-f.



a. deploying b. moving to the right c. grasping d. moving to the left e. releasing f. retracting

Figure 12. Grasp the right object and release it to the left box.

The above pick-and-place experiments validate motion feasibility of this kind of mechanism. The end drive assembly and the middle drive assembly can effectively control the position of the gripper. And the steering motor under the middle drive assembly can well control the orientation of the gripper. The motion experiments verify the correctness of the previous design and analysis.

Since the planar parallel manipulator with tape spring has low masses, simple mechanics and high efficiency of enfoldment, this manipulator is very suitable for use on some small platform, e.g., a UAV (unmanned aerial vehicle). During the course of the UAV takeoff, flight, or landing, the manipulator can be compacted to a stowed configuration under the UAV. When in operating mode, the manipulator extends to a deployed configuration and executes the task.

7. Conclusion

In this paper, a novel deployable planar parallel manipulator with tape spring mechanism has been proposed. The manipulator has low masses, simple mechanics and high efficiency of enfoldment. The detailed design of this deployable planar parallel manipulator has been presented. The kinematic model is derived, and the singularity of this mechanism is discussed. Then, the simplified dynamic model is established. Within consideration of buckling stability of the tape spring, the workspace of the moving platform is investigated. The torques of the two driving pulleys are studied. And the distributions of the driving torque in the workspace are figured out. At last, the prototype is manufactured. The pick-and-place experiments are tested to validate the presented design and analysis. And potential application of the deployable parallel manipulator for UAV is discussed.

Acknowledgements

This research has been supported by the National Natural Science Foundation of China under Grant 51675318, 91748116, 91648119.

References

- [1] Z. You, S. Pellegrino, Foldable bar structures, *Int. J. Solids Struct.* 34 (15) (1997), 1825–1847.
- [2] G. Kiper, E. Söylemez, A.Ö. Kisisel, A family of deployable polygons and polyhedra, *Mechanism and Machine Theory*, 43 (5) (2008), 627–640.
- [3] X. Ding, Y. Yang, J.S. Dai, Design and kinematic analysis of a novel prism deployable mechanism, *Mechanism and Machine Theory*, 63 (2013), 35–49.
- [4] Y. Chen, Design of structural mechanisms, University of Oxford, 2003.
- [5] Shengnan Lyu, Dimiter Zlatanov, Matteo Zoppi, Xilun Ding, Gregory S. Chirikjian, and Simon D. Guest, Bundle folding type III Bricard linkages, *Mechanism and Machine Theory*, 144 (2020): 103663.
- [6] W. Zhang, S. Lu, X. Ding, Recent development on innovation design of reconfigurable mechanisms in China, *Frontiers of Mechanical Engineering*, (2019), 14(1):15-20.
- [7] J.S. Dai, D. Wang, L. Cui, Orientation and workspace analysis of the multifingered metamorphic hand—metahand, *IEEE Trans, Robot*, 25 (4) (2009), 942–947.
- [8] D. Chablat, L. Rolland, Design of mechanisms with scissor linear joints for swept volume reduction, The 4th Joint International Conference on Multi-body System Dynamics, 2016.
- [9] D.J. Gonzalez, H.H. Asada, Design and analysis of 6-dof triple scissor extender robots with applications in aircraft assembly, *IEEE Robot, Autom, Lett.* 2 (3) (2017), 1420–1427.
- [10] Y. Yang, Y. Tian, Y. Peng, H. Pu, A novel 2-DOF planar translational mechanism composed by scissor-like elements, *Mechanical Science*, 8 (1) (2017), 179–193.
- [11] Y. Yang, Y. Peng, H. Pu, H. Chen, X. Ding, G.S. Chirikjian, S. Lyu, Deployable parallel lower-mobility manipulators with scissor-like elements, *Mechanism and Machine Theory*, (2019), 135, 226–250.
- [12] de Jong, M. G., van de Sande, W. W., & Herder, J. L., Properties of two-fold tape loops: the influence of the subtended angle, *Journal of Mechanisms and Robotics*, (2019), 11(2), 020912.
- [13] Calladine, C. R., The theory of thin shell structures 1888-1988, *Institution of Mechanical Engineers*, (1988), 202(A3), pp. 141–149.
- [14] Seffen, K. A., and Pellegrino, S., Deployment dynamics of tape springs, *The Royal Society*, (1999), 455, pp. 1003–1048.